Eur. Phys. J. C 53, 615–620 (2008)
DOI 10.1140/epjc/s10052-007-0492-3

THE EUROPEAN PHYSICAL JOURNAL C

Regular Article – Theoretical Physics

Pair production of charged Higgs bosons in the left–right twin Higgs model at the ILC and LHC

Yao-Bei Liu[1,a], Hong-Mei Han[1], Xue-Lei Wang[2]

[1] School of Machinery and Electricity, Henan Institute of Science and Technology, Xinxiang 453003, P.R. China
[2] College of Physics and Information Engineering, Henan Normal University, Xinxiang 453007, P.R. China

Received: 1 June 2007 / Revised version: 24 November 2007 /
Published online: 22 December 2007 –

Abstract. The left–right twin Higgs (LRTH) model predicts the existence of a pair of charged Higgs bosons $\phi^{\pm}$. In this paper, we study the production of the charged Higgs boson pair $\phi^{\pm}$ at the international linear collider (ILC) and the CERN large hadron collider (LHC). The numerical results show that the production rates are at the level of several tens fb at the ILC, and the process $e^+e^- \to \phi^+\phi^-$ can produce adequately distinct multi-jet final states. We also discuss the charged Higgs boson pair production via the process $q\bar{q} \to \phi^+\phi^-$ at the LHC and estimate in this case the production rates. We find that, as long as the charged Higgs bosons are not too heavy, they can be abundantly produced at the LHC. The possible signatures of these new particles might be detected at the ILC and LHC experiments.

PACS. 12.60.Fr; 14.80.Mz; 14.65.Ha; 12.15.Lk

1 Introduction

The standard model (SM) provides an excellent effective field theory description of almost all particle physics experiments. But in the SM the Higgs boson mass suffers from an instability under radiative corrections. The naturalness argument suggests that the cutoff scale of the SM is not much above the electroweak scale: new physics will appear around TeV energies. Most extensions of the SM require the introduction of an extended Higgs sector into the theory. Generically, a charged Higgs boson that does not exist in the SM arises in the extended Higgs sector. It implies that the observation of a charged Higgs boson is clear evidence for the existence of new physics beyond the SM. Many alternative new physics theories, such as supersymmetry, topcolor, and the little Higgs model predict the existence of new scalar or pseudo-scalar particles. These new particles may have cross sections and branching fractions that differ from those of the SM Higgs boson. Thus, studying the production and decays of the new scalars at high energy colliders will be of special interest.

Recently, the twin Higgs mechanism has been proposed as a solution to the little hierarchy problem [1–4]. The Higgs is a pseudo-Goldstone boson of a spontaneously broken global symmetry. Gauge and Yukawa interactions that explicitly break the global symmetry give mass to the Higgs boson. Once a discrete symmetry is imposed, the leading quadratic divergent term respects the global symmetry, and it thus does not contribute to the Higgs model. The twin Higgs mechanism can be implemented in left–right models with the discrete symmetry being identified with left–right symmetry [3]. The left–right twin Higgs (LRTH) model contains the $\mathrm{U}(4)_1 \times \mathrm{U}(4)_2$ global symmetry as well as the $\mathrm{SU}(2)_\mathrm{L} \times \mathrm{SU}(2)_\mathrm{R} \times \mathrm{U}(1)_{\mathrm{B-L}}$ gauge symmetry. The left–right symmetry acts only on the two-SU(2) gauge symmetry. The leading quadratically divergent SM gauge boson contributions to the Higgs masses are canceled by the loop involving the heavy gauge bosons. A vector top singlet pair is introduced to generate an $\mathcal{O}(1)$ top Yukawa coupling. The quadratically divergent SM top contributions to the Higgs potential are canceled by the contributions from a heavy top partner. The LRTH model predicted the existence of new heavy particles such as heavy gauge boson, fermions, and scalars at or below the TeV scale that might generate characteristic signatures at the present and future collider experiments [5–10].

The hunt for the Higgs boson and the elucidation of the mechanism of symmetry breaking is one of the most important goals for present and future high energy collider experiments. Precision electroweak measurement data and direct searches suggest that the Higgs boson must be relatively light and its mass should be roughly in the range of 114.4–208 GeV at 95% CL [11, 12]. While the discovery potential of the Higgs boson at the LHC has been established for a wide range of Higgs masses, only rough estimates of its properties will be possible, through measurements on the couplings of the Higgs particle to the fermions and gauge boson for example [13, 14]. The most precise measurements will be performed in the clean environment of the future high energy e^+e^- linear collider, the interna-

[a] e-mail: hnxxlyb2000@sina.com

tional linear collider (ILC) with the center of mass (c.m.) energy $\sqrt{s} = 300$ GeV–1.5 TeV [15] and a yearly luminosity of 500 fb^{-1}. The running of the high energy and luminosity linear collider will open an unique window for us to reach understanding of the fundamental theory of particle physics. The aim of this paper is to investigate production of the charged Higgs boson pair at the ILC and LHC and see whether the possible signatures of the LRTH model can be detected in the near future ILC and LHC experiments.

This paper is organized as follows, The relevant couplings to ordinary particles of the charged Higgs bosons $\phi^{\pm}$ in the LRTH model are given in Sect. 2. In Sects. 3 and 4 we study the charged Higgs bosons pair productions at the ILC and LHC, respectively. The numerical results and discussions are also presented in these sections. The conclusions are given in Sect. 5.

2 The relative couplings

The LRTH model is based on the global $\mathrm{U}(4)_1 \times \mathrm{U}(4)_2$ symmetry, with a locally gauged subgroup $\mathrm{SU}(2)_\mathrm{L} \times \mathrm{SU}(2)_\mathrm{R} \times \mathrm{U}(1)_{\mathrm{B-L}}$. Two Higgs fields, H and $\hat{H}$, are introduced and each transforms as $(4,1)$ and $(1,4)$ respectively under the global symmetry. They are written

$$H = \begin{pmatrix} H_\mathrm{L} \\ H_\mathrm{R} \end{pmatrix}, \quad \hat{H} = \begin{pmatrix} \hat{H}_\mathrm{L} \\ \hat{H}_\mathrm{R} \end{pmatrix}, \tag{1}$$

where $H_\mathrm{L,R}$ and $\hat{H}_\mathrm{L,R}$ are two component objects that are charged under $\mathrm{SU}(2)_\mathrm{L} \times \mathrm{SU}(2)_\mathrm{R} \times \mathrm{U}(1)_{\mathrm{B-L}}$ as follows:

$$H_\mathrm{L} \text{ and } \hat{H}_\mathrm{L}: \quad (2,1,1), \qquad H_\mathrm{R} \text{ and } \hat{H}_\mathrm{R}: \quad (1,2,1). \tag{2}$$

The global $\mathrm{U}(4)_1(\mathrm{U}(4)_2)$ symmetry is spontaneously broken down to its subgroup $\mathrm{U}(3)_1(\mathrm{U}(3)_2)$ with non-zero vacuum expectation values as $\langle H \rangle = (0,0,0,f)$ and $\langle \hat{H} \rangle = (0,0,0,\hat{f})$. Each spontaneous symmetry breaking results in seven Nambu–Goldstone bosons. Three of six Goldstone bosons that are charged under $\mathrm{SU}(2)_\mathrm{R}$ are eaten by the heavy gauge bosons, while this leaves three physical Higgs particles: ϕ^0 and $\phi^{\pm}$. The remaining Higgs particles are the SM Higgs doublet H_L and an extra Higgs doublet, $\hat{H}_\mathrm{L} = (\hat{H}_1^+, \hat{H}_2^0)$, which only couples to the gauge boson sector. A residue matter parity in the model renders the neutral Higgs $\hat{H}_2^0$ stable, and it could be a good dark matter candidate. A pair of vector-like quarks, q_L and q_R, are introduced in order to give the top quark a mass of the order of the electroweak scale; these are singlets under $\mathrm{SU}(2)_\mathrm{L} \times \mathrm{SU}(2)_\mathrm{R}$. The masses of the light SM-like top and the heavy top are [5]

$$m_t^2 \simeq y^2 f^2 \sin^2 x - M^2 \sin^2 x \sim (yv/\sqrt{2})^2, \tag{3}$$
$$m_T^2 \simeq y^2 f^2 + M^2 - m_t^2, \tag{4}$$

where $v = 246$ GeV is the electroweak scale and $x = v/\sqrt{2}f$; the mass parameter M is essential to the mixing between the SM-like top quark and the heavy top quark. The top Yukawa coupling can then be determined by fitting the experimental value of the light top quark mass. At the leading order of $1/f$, the mixing angles for left-handed and right-handed fermions are [5]

$$S_\mathrm{L} \simeq \frac{M}{m_T} \sin x, \tag{5}$$
$$S_\mathrm{R} \simeq \frac{M}{m_T} \left(1 + \sin^2 x\right). \tag{6}$$

The value of M is constrained by the requirement that the branching ratio of $Z \to b\bar{b}$ remains consistent with the experiments. We define the Weinberg angle in the LRTH model as

$$s_\mathrm{W} = \sin\theta_w = \frac{g'}{\sqrt{g^2 + 2g'^2}}, \tag{7}$$
$$c_\mathrm{W} = \cos\theta_w = \sqrt{\frac{g^2 + g'^2}{g^2 + 2g'^2}}. \tag{8}$$

The unit of the electric charge is then given by

$$e = g s_\mathrm{W} = \frac{gg'}{g^2 + 2g'^2}. \tag{9}$$

The LRTH model introduces new charged Higgs bosons $\phi^{\pm}$ in addition to the neutral Higgs ϕ^0 and the SM Higgs boson h. For the neutral gauge bosons, we write the couplings to the fermions in the form $i\gamma^\mu(g_\mathrm{V} + g_\mathrm{A}\gamma^5)$. The coupling constants of the heavy gauge bosons and the charged Higgs boson $\phi^{\pm}$ to ordinary particles, which are related to our calculation, can be written [5]

$$g_\mathrm{V}^{Z_H \bar{e}e} = \frac{e}{4 s_\mathrm{W} c_\mathrm{W} \sqrt{1 - 2s_\mathrm{W}^2}} \left(-1 + 4s_\mathrm{W}^2\right),$$
$$g_\mathrm{A}^{Z_H \bar{e}e} = -\frac{e}{4 s_\mathrm{W} c_\mathrm{W}} \sqrt{1 - 2s_\mathrm{W}^2}, \tag{10}$$
$$g_\mathrm{V}^{Z_H \bar{u}_{1,2} u_{1,2}} = \frac{e}{4 s_\mathrm{W} c_\mathrm{W} \sqrt{1 - 2s_\mathrm{W}^2}} \left(-1 + \frac{8}{3} s_\mathrm{W}^2\right),$$
$$g_\mathrm{A}^{Z_H \bar{u}_{1,2} u_{1,2}} = -\frac{e}{4 s_\mathrm{W} c_\mathrm{W}} \sqrt{1 - 2s_\mathrm{W}^2}, \tag{11}$$
$$g_\mathrm{V}^{Z_H \bar{d}_{1,2} d_{1,2}} = \frac{e}{4 s_\mathrm{W} c_\mathrm{W} \sqrt{1 - 2s_\mathrm{W}^2}} \left(1 - \frac{5}{3} s_\mathrm{W}^2\right),$$
$$g_\mathrm{A}^{Z_H \bar{d}_{1,2} d_{1,2}} = \frac{e}{4 s_\mathrm{W} c_\mathrm{W}^3 \sqrt{1 - 2s_\mathrm{W}^2}}, \tag{12}$$
$$g_\mathrm{V}^{Z_H \bar{b}b} = \frac{e}{4 s_\mathrm{W} c_\mathrm{W} \sqrt{1 - 2s_\mathrm{W}^2}} \left(1 - \frac{4}{3} s_\mathrm{W}^2\right),$$
$$g_\mathrm{A}^{Z_H \bar{b}b} = \frac{e}{4 s_\mathrm{W} c_\mathrm{W}} \sqrt{1 - 2s_\mathrm{W}^2}, \tag{13}$$
$$g^{\phi^-\phi^+\gamma} = -e(p_1 - p_2)_\mu,$$
$$g^{\phi^-\phi^+Z} = \frac{e s_\mathrm{W}}{c_\mathrm{W}} (p_1 - p_2)_\mu, \tag{14}$$
$$g^{\phi^-\phi^+Z_H} = -\frac{e\left(1 - 3s_\mathrm{W}^2\right)}{2 s_\mathrm{W} c_\mathrm{W} \sqrt{1 - 2s_\mathrm{W}^2}} (p_1 - p_2)_\mu,$$
$$g^{\phi^+\bar{t}b} = -\mathrm{i}\left(S_\mathrm{R} m_b P_\mathrm{L} - y S_\mathrm{L} f P_\mathrm{R}\right)/f, \tag{15}$$

where $P_{\mathrm{L(R)}} = (1 \mp \gamma_5)/2$ is the left- (right-) handed projection operator. s_W (c_W) represents the sine (cosine) of the Weinberg angle, and p_1 and p_2 refer to the incoming momentum of the first and second particle, respectively.

3 Production of the charged Higgs bosons pair at ILC

From the above discussions, we can see that the charged Higgs boson pair $\phi^+\phi^-$ can be produced in e^+e^- annihilation via virtual photon or neutral gauge boson exchange. The Feynman diagram of the process $e^+e^- \to \phi^+\phi^-$ is shown in Fig. 1.

At the leading order, the production amplitude of the process can be written as

$$\mathcal{M}_1 = \mathcal{M}_\gamma + \mathcal{M}_Z + \mathcal{M}_{Z_H} , \tag{16}$$

with

$$\begin{aligned}
\mathcal{M}_\gamma &= e^2 \overline{v}_e(p_2)\gamma^\mu u_e(p_1) G^{\mu\nu}(p_1+p_2,0)(p_3-p_4)_\nu , \\
\mathcal{M}_Z &= \frac{e s_\mathrm{W}}{c_\mathrm{W}} \overline{v}_e(p_2)\gamma^\mu \left(g_\mathrm{V}^{Z\bar{e}e} + _\mathrm{A}^{Z\bar{e}e}\gamma^5\right) u_e(p_1) \\
&\quad \times G^{\mu\nu}(p_1+p_2, M_Z)(p_3-p_4)_\nu , \\
\mathcal{M}_{Z_H} &= \frac{e\left(1-3s_\mathrm{W}^2\right)}{2 s_\mathrm{W} c_\mathrm{W}\sqrt{1-2s_\mathrm{W}^2}} \overline{v}_e(p_2)\gamma^\mu \\
&\quad \times \left(g_\mathrm{V}^{Z_H\bar{e}e} + _\mathrm{A}^{Z_H\bar{e}e}\gamma^5\right) u_e(p_1) \\
&\quad \times G^{\mu\nu}\left(p_1+p_2, M_{Z_H}\right)(p_3-p_4)_\nu .
\end{aligned}$$

Here, $G^{\mu\nu}(p,M) = \frac{-\mathrm{i}g^{\mu\nu}}{p^2-M^2}$ is the propagator of the particle. With the above production amplitudes, we can obtain the production cross section directly. In the calculation of the cross section, instead of calculating the square of the amplitudes analytically, we calculate the amplitudes numerically by using the method of [16, 17], which can greatly simplify our calculation.

In the numerical calculation, we take the input parameters as $G_\mathrm{F} = 1.166\times10^{-5}\,\mathrm{GeV}^{-2}$, $M_Z = 91.187$ GeV and $s_\mathrm{W}^2 = 0.2315$ [18]. The electromagnetic fine-structure constant α_e at a certain energy scale is calculated from the simple QED one-loop evolution with the boundary value $\alpha_e = 1/137.04$. Except for these SM input parameters, the production cross sections is dependent on the symmetry breaking f, the mixing parameter M and the mass of the charged Higgs boson $\phi^\pm$. In our analysis, we take M to be small and pick a typical value of $M = 150$ GeV. The symmetry breaking scale f is allowed in the range of 500–1500 GeV [5]. As numerical estimation, we will assume that $M_{\phi^\pm}$ is in the range of 150–450 GeV.

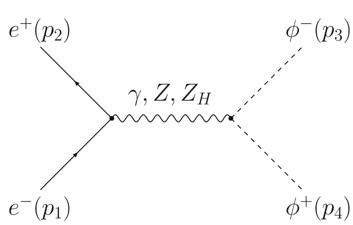

Fig. 1. Feynman diagrams of the process $e^+e^- \to \phi^+\phi^-$

In Fig. 2, we plot the cross section of $e^+e^- \to \phi^+\phi^-$ as a function of the mass parameter $M_{\phi^\pm}$ for $M_{Z_H} = 2.5$ TeV and three values of the center of mass energy. The plots show that the cross section decreases with $M_{\phi^\pm}$, due to phase space suppression. For $\sqrt{s} = 500$ GeV, the cross section falls sharply to a very small rate with $M_{\phi^\pm}$ increasing. So, the energy 500 GeV is not suitable to search for the heavy charged Higgs bosons pair. The cross section is not sensitive to $M_{\phi^\pm}$ when $\sqrt{s} = 1600$ GeV. The change of the cross section with $\sqrt{s}$ is not monotonous because the influence of $\sqrt{s}$ on the phase space and the Z-propagator is inverse. In the cases, the production rate is at the order of tens fb. For the light charged scalars, the production rate can be near 30 fb in the case of $\sqrt{s} = 800$ GeV. With a yearly expected luminosity about £ $= 500\,\mathrm{fb}^{-1}$, there will be 10^2–10^4 events to be generated each year.

To see the influence of the new heavy gauge boson mass M_{Z_H} on the cross section, in Fig. 3 we plot $\sigma(s)$ as a function of M_{Z_H} for $\sqrt{s} = 800$ GeV and three values of $M_{\phi^\pm} = 150$, 250 and 350 GeV, respectively. From Fig. 3, one can see that the cross section decreases slowly with M_{Z_H} increasing and is more sensitive to the charged Higgs bosons mass. This is because the production cross section are mainly aroused by the exchange of γ and Z boson. In general, the cross section is at the order of tens fb. This abundant production allows one to enforce tight requirements on the event pre-selection and the mass reconstruction.

It has been shown that the charged Higgs $\phi^\pm$ dominantly decay into tb for larger value of the mixing parameter between the SM-like top quark and the heavy top quark [5]. In the case of $\phi^+ \to t\bar{b}$, the signal of the charged Higgs bosons pair production is $t\bar{t}b\bar{b}$. The cross section of the irreducible $t\bar{t}b\bar{b}$ background has been estimated using the Comphep program [19] at 0.8 TeV and has been found to be 5.5 fb. In order to efficiently distinguish the signals from the underlying backgrounds and to measure

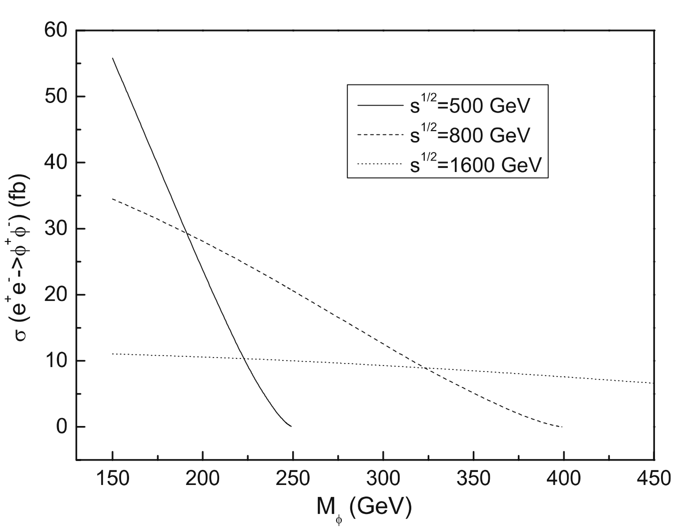

Fig. 2. The cross section of $e^+e^- \to \phi^+\phi^-$ as a function of the charged Higgs bosons mass $M_{\phi^\pm}$ for $f = 1$ TeV, $M = 150$ GeV and various center-of-mass values $\sqrt{s}$

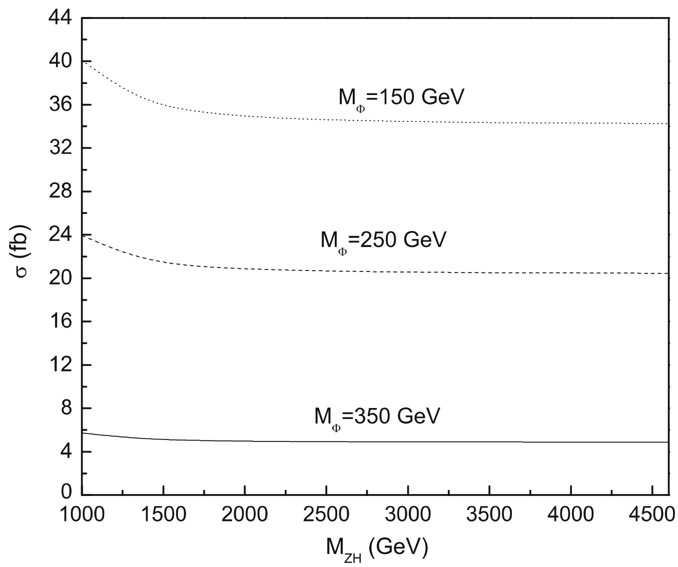

Fig. 3. The cross section $\sigma(s)$ of $e^+e^- \to \phi^+\phi^-$ as a function of the heavy gauge boson mass M_{Z_H} for $\sqrt{s} = 800$ GeV and various values of $M_{\phi^\pm}$

the charged scalar mass, it is important to obtain a clean charged scalar signal in the mass distribution of the multi-jet final states. To identify the production mode $t\bar{t}b\bar{b}$, we insist on eight jets or one lepton plus six jets (in particular, fewer than ten visible lepton/jets so as to discriminate from the $4t$ final states) and possibly require that one W and the associated top quark be reconstructed. In particular, since the final states contain at least four b jets, in order to eliminate any residual QCD background, we need one or two b-tags without incurring significant penalty. Such b-tagging should have the efficiency of 60% or better. The mistagging of b-quark and s-quark will make the $e^+e^- \to W^+W^-$ important, which significantly enhances the background. So, the efficient b-tagging and mass reconstruction of the charged Higgs bosons is very necessary to reduce the background [20].

It is known that many new physics models predict similar heavy charged scalars, such as $\Pi^\pm$ in the topcolor-assisted technicolor model (TC2) and $H^\pm$ in the two-Higgs doublet model (2HDM). To distinguish the scalars in the LRTH model from the charged top-pions in the TC2 model and the Higgs bosons in the 2HDM, we should compare the cross section of $e^+e^- \to \phi^+\phi^-$ with those of the similar process $e^+e^- \to \Pi^+\Pi^-$ [21] in the TC2 model and the process $e^+e^- \to H^+H^-$ [22, 23] in the 2HDM. The cross section values of processes such as these three are not significantly different for the same parameters. For example, $\sigma(e^+e^- \to \Pi^+\Pi^-) = 21.51, 15.09\,\text{fb}$ with $\sqrt{s} = 800, 1600\,\text{GeV}$ and $M_\Pi = 300\,\text{GeV}$, $\sigma(e^+e^- \to H^+H^-) = 10.02, 8.1\,\text{fb}$ with $\sqrt{s} = 800, 1600\,\text{GeV}$ and $M_H = 300\,\text{GeV}$, $\sigma(e^+e^- \to \phi^+\phi^-) = 12.54, 9.26\,\text{fb}$ with $\sqrt{s} = 800, 1600\,\text{GeV}$ and $M_\phi = 300\,\text{GeV}$. So we should distinguish them depending on their different features of decay modes and pole structure. The $t\bar{b}$ is the main decay mode for the charged scalars. However, we should probe charged top-pions via the flavor-changing decay mode $\Pi^+ \to c\bar{b}$ to obtain the identified signals. $\tau\nu_\tau$ can also provide the identified signals of charged Higgs from the 2HDM, which does not exist for the charged top-pions and $\phi^\pm$.

4 Production of the charged Higgs bosons pair at LHC

The large hadron collider (LHC) at CERN has a good potential for the discovery of a charged Higgs boson. At the LHC, the charged Higgs bosons also can be produced in pair production mode. There are two important $\phi^+\phi^-$ production channels: (i) $q\bar{q} \to \phi^+\phi^-$, where $(q = u, d, c, s, b)$ (via the Drell–Yan process, where a photon and a Z boson are exchanged in the s-channel and the top quark in the t-channel) [24]; (ii) the loop-induced gluon fusion process $gg \to \phi^+\phi^-$ [25–28]. The Feynman diagrams of these processes are shown in Fig. 4. In the case of $q = b$, there are additional Feynman diagrams involving ϕ^0 and H in Fig. 4a, the neutral Higgs bosons ϕ^0 and H exchange in the s-channel can also contribute to the pair production process. However, these contributions are very much smaller than those of the other tree-level processes because of either the small Yukawa couplings, the small parton distribution functions or both combined. On the other hand, the contributions from Fig. 4c–e are also very much smaller than those of the tree-level processes. This is because the Yukawa couplings depend sensitively on the parameter M and f. For small f, the values of the parameter M are very small [6]. Once M is very small or in the limit that $M = 0$, certain couplings go to zero. Although the gluon fusion get an enhancement due to larger parton distribution

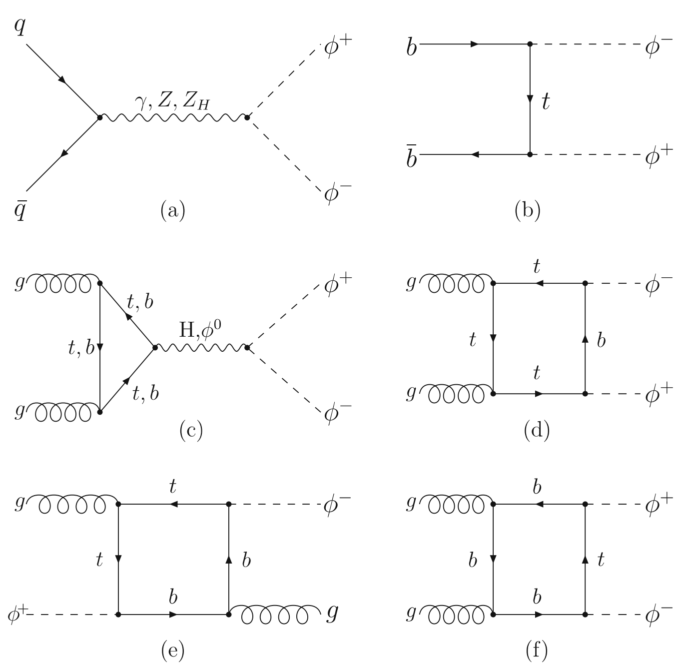

Fig. 4. Tree-level Feynman diagrams for the process $q\bar{q} \to \phi^+\phi^-$ (**a**,**b**) and one-loop Feynman diagrams for $gg \to \phi^+\phi^-$ (**c**–**f**) in the LRTH model

functions, the contributions of gluon fusion process is suppressed by the order of $(M/f)^4$. Thus, we will ignore these processes in the following estimation.

Using the relevant Feynman rules, we can write the invariant amplitude for the parton process $q(p_1)\bar{q}(p_2) \to \phi^+(p_3)\phi^-(p_4)$ as

$$\mathcal{M}_2 = \mathcal{M}_{21} + \mathcal{M}_{22}\,. \tag{17}$$

For the process $b\bar{b} \to \phi^+\phi^-$, the invariant amplitude comes from Fig. 4a and b:

$$\begin{aligned}
\mathcal{M}_{21} = {} & e\bar{v}\,(p_2)\,Q\gamma_\nu u(p_1) g^{\mu\nu}\,(p_4-p_3)_\mu \\
& + \frac{es_{\mathrm{W}}}{c_{\mathrm{W}}}\bar{v}\,(p_2)\,\gamma_\nu\left(g_{\mathrm{V}}^{Zb\bar{b}} + g_{\mathrm{A}}^{Zb\bar{b}}\gamma_5\right) \\
& \times u(p_1)\frac{g^{\mu\nu}}{\hat{s}-m_Z^2}\,(p_4-p_3)_\mu \\
& + \frac{e\left(1-3s_{\mathrm{W}}^2\right)}{2c_{\mathrm{W}}s_{\mathrm{W}}\sqrt{1-2s_{\mathrm{W}}^2}}\bar{v}(p_2)\gamma_\nu\left(g_{\mathrm{V}}^{Z_H b\bar{b}} + g_{\mathrm{A}}^{Z_H b\bar{b}}\gamma_5\right) \\
& \times u(p_1)\frac{g^{\mu\nu}}{\hat{s}-m_{Z_H}^2}\,(p_4-p_3)_\mu \\
& + \frac{1}{f^2}\bar{v}\,(p_2)\,(S_{\mathrm{R}} m_b P_{\mathrm{L}} - yS_{\mathrm{L}} f P_{\mathrm{R}})\,\frac{\not{q}+m_t}{\hat{t}-m_t^2} \\
& \times (S_{\mathrm{R}} m_b P_{\mathrm{R}} - yS_{\mathrm{L}} f P_{\mathrm{L}})\,u(p_1)\,.
\end{aligned} \tag{18}$$

For u, c, d, c and s quarks, we only consider the contributions of the s-channel process to the scattering amplitude, which can be written

$$\begin{aligned}
\mathcal{M}_{22} = {} & e\bar{v}(p_2)Q\gamma_\nu u(p_1)g^{\mu\nu}(p_4-p_3)_\mu \\
& + \frac{es_{\mathrm{W}}}{c_{\mathrm{W}}}\bar{v}(p_2)\gamma_\nu\left(g_{\mathrm{V}}^{Zq\bar{q}} + g_{\mathrm{A}}^{Zq\bar{q}}\gamma_5\right) \\
& \times u(p_1)\frac{g^{\mu\nu}}{\hat{s}-m_Z^2}(p_4-p_3)_\mu \\
& + \frac{e\left(1-3s_{\mathrm{W}}^2\right)}{2c_{\mathrm{W}}s_{\mathrm{W}}\sqrt{1-2s_{\mathrm{W}}^2}}\bar{v}(p_2)\gamma_\nu\left(g_{\mathrm{V}}^{Z_H q\bar{q}} + g_{\mathrm{A}}^{Z_H q\bar{q}}\gamma_5\right) \\
& \times u\,(p_1)\,\frac{g^{\mu\nu}}{\hat{s}-m_{Z_H}^2}(p_4-p_3)_\mu\,,
\end{aligned} \tag{19}$$

with $Q = 2e/3$ (for $q = u, c$) and $Q = -e/3$ (for $q = d, s, b$). Here $\hat{s} = (p_1+p_2)^2$ and $\hat{t} = (p_1-p_3)^2$ are the usual Mandelstam variables. We have neglected the light quark masses in our calculations except for the bottom quark. From the above equations, we can see that the production cross section of the t-channel process is suppressed by the order of $(M/f)^4$. Furthermore, the cross section via the new heavy gauge boson Z_H exchange is suppressed by an order of magnitude compared to that for the s-channel Z exchange and photon exchange. Therefore, the main production processes are the usual Drell–Yan processes through the s-channel Z exchange and photon exchange.

To get the numerical results, we take the input parameter $m_t = 172.7$ GeV [29] and we used the CTEQ6L parton distribution functions [30] and the two-loop running coupling constant $\alpha_{\mathrm{s}}(m_Z) = 0.118$. There are two free parameters: f and the value of the mixing parameter M. In this paper, we will take the typical values of $f = 1000$ GeV and $M = 150$ GeV. Our numerical results are shown in Fig. 5, in which we plot the production cross section $\sigma(\phi^+\phi^-)$ for the process $p\bar{p} \to \phi^+\phi^- + X$ at the LHC with $\sqrt{s} = 14$ TeV as a function of the charged Higgs bosons mass $M_{\phi^\pm}$ for $f = 1000$ GeV. For comparison, we use the solid line and dashed line to represent the contributions of the process $q\bar{q} \to \phi^+\phi^-(q = u,\ d,\ c,$ and $s)$ and the process $b\bar{b} \to \phi^+\phi^-$, respectively. From Fig. 5 one can see that the production cross section of the charged Higgs bosons $\phi^+\phi^-$ mainly comes from the usual Drell–Yan processes $q\bar{q} \to \phi^+\phi^-$ $(q = u, d, c,$ and $s)$ through the s-channel gauge bosons exchange and photon exchange. The total production cross section $\sigma(\phi^+\phi^-)$ is in the range of 134.5–1.7 fb for 150 GeV $\le M_{\phi^\pm} \le$ 450 GeV. The charged top-pions pair in the Higgsless-top-Higgs (HTH) model and charged Higgs bosons in the minimal supersymmetry standard model (MSSM) pair production at the LHC have been calculated to leading and next-to-leading order [31–35]. They have shown that the total cross section for the charged top-pions and Higgs boson pair production processes is smaller than 10 fb in most of the parameter space. Thus, we expected that the charged Higgs bosons $\phi^+\phi^-$ predicted by the LRTH model can be more easy detected at the LHC via this process than those for the charged top-pions $\pi^\pm$ in the HTH model and charged Higgs bosons $H^\pm$ in the MSSM.

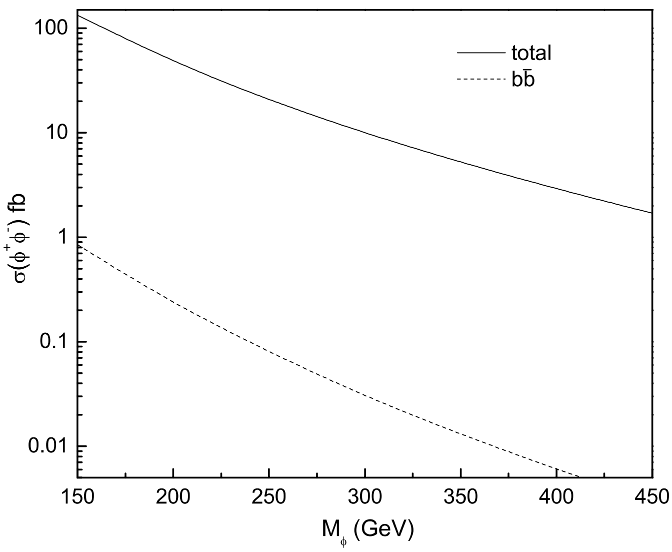

Fig. 5. The cross section of the process $q\bar{q} \to \phi^+\phi^-$ as a function of the charged Higgs bosons mass $M_{\phi^\pm}$ for $f = 1000$ GeV and $M = 150$ GeV

5 Conclusions

The SM predicts the existence of a neutral Higgs boson, while many popular models beyond the SM predict the existence of neutral or charged scalar particles. These new particles might produce observable signatures in the current or future high energy experiments different from the case of the SM Higgs boson. Any visible signal from the new scalar particles will be evidence of new physics beyond the SM. Thus, studying the new scalar particle production is very interesting at the ILC and LHC.

The twin Higgs mechanism provides an alternative method to solve the little hierarchy problem. The LRTH model is a concrete realization of the twin Higgs mechanism. The cancellation of divergences occurs by alignment of vacua and the existence of several new particles. The new particles in the LRTH model are the heavy top quark, new gauge bosons, and new Higgs bosons, which might produce characteristic signatures at the ILC and LHC experiments.

In this paper, we discuss the pair production of the charged Higgs bosons $\phi^+\phi^-$ predicted by the LRTH model at the ILC and the LHC via suitable mechanisms. We can obtain the following conclusions. (i) For the production of $\phi^+\phi^-$ at the ILC, we found that the production rate is at the level of several tens fb in a large part of the parameter space. Efficient b-tagging and mass reconstruction of the charged Higgs bosons is needed in order to reduce the background. We concluded that the charged scalars $\phi^\pm$ predicted by the LRTH model should be experimentally observable via the process $e^+e^- \to \phi^+\phi^-$ at the ILC. (ii) For the production of $\phi^+\phi^-$ at the LHC, we found that the total production cross section $\sigma(\phi^+\phi^-)$ is in the range of 134.5–1.7 fb for 150 GeV $\leq M_{\phi^\pm} \leq$ 450 GeV, which might be larger than those for the charged top-pions $\pi^\pm$ in the HTH model and charged Higgs bosons $H^\pm$ in the MSSM. The main production processes are the usual Drell–Yan processes through the s-channel Z exchange and photon exchange. In conclusion, as long as the charged Higgs bosons is not too heavy, we conclude that the pair production of the charged Higgs bosons will be a good test for the LRTH model at future ILC and LHC experiments.

Acknowledgements. This work is supported in part by the National Natural Science Foundation of China (Grant No. 10775039 and 10575029) and a grant from Henan Institute of Science and Technology (06040).

References

1. Z. Chacko, H.S. Goh, R. Harnik, Phys. Rev. Lett. **96**, 231 802 (2006)
2. Z. Chacko, Y. Nomura, M. Papucci, G. Perez, JHEP **0601**, 126 (2006)
3. Z. Chacko, H.S. Goh, R. Harnik, JHEP **0601**, 108 (2006)
4. A. Falkowski, S. Pokorski, M. Schmaltz , Phys. Rev. D **74**, 035 003 (2006)
5. H.-S. Goh, S. Su, Phys. Rev. D **75**, 075 010 (2007)
6. D.-W. Jung, J.-Y. Lee, hep-ph/0701071
7. Y.-B. Liu, H.-M. Han, Y.-H Cao, hep-ph/0703268
8. Y.-B. Liu, J.-F. Shen, 0704.0840 [hep-ph]
9. H.-S. Goh, C.A. Krenke, 0707.3650 [hep-ph]
10. A. Abada, I. Hidalgo, 0711.1238 [hep-ph]
11. M.W. Grunewald, in: Proc. of the Workshop on Electroweak Precision Data and the Higgs Mass, hep-ex/0304023
12. LEP Collaboration, LEP Electroweak Working Group, SLD Heavy Flavour Group, hep-ex/0412015
13. ATLAS Collaboration, Technical Design Report, CERN-LHCC-99-15
14. LHC/LC Study Group, G. Weiglein et al., hep-ph/0410364
15. ACFA Linear Collider Working Group, K. Abe et al., hep-ph/0109166
16. K. Hagiwara, D. Zeppenfeld, Nucl. Phys. B **313**, 560 (1989)
17. V. Barger, T. Han, D. Zeppenfeld, Phys. Rev. D **41**, 2782 (1990)
18. Particle Data Group, W.M. Yao et al., J. Phys. G **33**, 1 (2006)
19. A. Pukhov et al., hep-ph/9908288
20. M. Battaglia, A. Ferrari, A. Kiiskinen, T. Maki, hep-ex/0112015
21. X.-L. Wang, Q.-P. Qiao, Q.-L. Zhang, Phys. Rev. D **71**, 095 012 (2005)
22. A. Djouadi, J. Kalinowski, P. Ohmanm, P.M. Zerwas, Z. Phys. C **74**, 93 (1997)
23. S. Moretti, Eur. Phys. J. C **34**, 157 (2004)
24. E. Eichten, I. Hinchliffe, K. Lane, C. Quigg, Rev. Mod. Phys. **56**, 579 (1984)
25. A.A.B. Bendezu, B.A. Kniehl, Nucl. Phys. B **568**, 305 (2000)
26. Y. Jiang, W.-G. Ma, L. Han, M. Han, Z.-H. Yu, J. Phys. G **24**, 83 (1998)
27. Y. Jiang, L. Han, W.-G. Ma, Z.-H. Yu, M. Han, J. Phys. G **23**, 385 (1997)
28. A. Belyaev, M. Drees, J.K. Mizukoshi, Eur. Phys. J. C **17**, 337 (2000)
29. CDF Collaboration, D0 Collaboration, Tevatron Electroweak Working group Combination of CDF and D0 results on the top quark mass, hep-ex/0507091
30. J. Pumplin et al., JHEP **0602**, 032 (2006)
31. C.-X. Yue, Y.-Q. Di, Nucl. Phys. B **762**, 55 (2006)
32. O. Brein, W. Hollik, Eur. Phys. J. C **13**, 175 (2000)
33. S. Moretti, J. Rathsman, Eur. Phys. J. C **33**, 41 (2004)
34. H.S. Hou et al., Phys. Rev. D **71**, 075 014 (2005)
35. A. Alves, T. Plehn, Phys. Rev. D **71**, 115 014 (2005)